

A New Approach to In-Situ “Micromanufacturing”: Microfluidic Fabrication of Magnetic and Fluorescent Chains Using Chitosan Microparticles as Building Blocks

Kunqiang Jiang, Chao Xue, Chanda Arya, Chenren Shao, Elijah O. George, Don L. DeVoe,* and Srinivasa R. Raghavan*

An in situ microfluidic assembly approach is described that can both produce microsized building blocks and assemble them into complex multiparticle configurations in the same microfluidic device. The building blocks are microparticles of the biopolymer chitosan, which is intentionally selected because its chemistry allows for simultaneous intraparticle and interparticle linking. Monodisperse chitosan-bearing droplets are created by shearing off a chitosan solution at a microfluidic T-junction with a stream of hexadecane containing a nonionic detergent. These droplets are then interfacially crosslinked into stable microparticles by a downstream flow of glutaraldehyde (GA). The functional properties of these robust microparticles can be easily varied by introducing various payloads, such as magnetic nanoparticles and/or fluorescent dyes, into the chitosan solution. The on-chip connection of such individual particles into well-defined microchains is demonstrated using GA again as the chemical “glue” and microchannel confinement as the spatial template. Chain flexibility can be tuned by adjusting the crosslinking conditions: both rigid chains and semiflexible chains are created. Additionally, the arrangement of particles within a chain can also be controlled, for example, to generate chains with alternating fluorescent and nonfluorescent microparticles. Such microassembled chains could find applications as microfluidic mixers, delivery vehicles, microscale sensors, or miniature biomimetic robots.

1. Introduction

The vision of “bottom-up” micromanufacturing involves manipulating and precisely positioning individual building blocks (subunits) into more complex, higher-order assemblies.^[1–16] For bottom-up microassembly to be realized

successfully, subunits have to be carefully defined, appropriate assembly methods must be chosen, and reliable techniques have to be developed for linking subunits together. In recent years, a variety of approaches have been put forward to produce microassemblies with defined geometries, patterns, compositions, and functional attributes.^[1–16] These studies have

K. Jiang
Departments of Chemistry & Biochemistry
University of Maryland
College Park, MD 20742, USA

C. Xue,^[+] C. Arya, E. O. George, Prof. S. R. Raghavan
Departments of Chemical & Biomolecular Engineering
University of Maryland
College Park, MD 20742, USA
E-mail: sraghava@umd.edu

C. Shao, Prof. D. L. DeVoe
Department of Mechanical Engineering
University of Maryland
College Park, MD 20742, USA
E-mail: ddev@umd.edu

[+] Current address: Department of Chemical Engineering, Massachusetts Institute of Technology, Cambridge, MA 02139, USA

DOI: 10.1002/sml.201100514

typically used prefabricated colloidal particles as the subunits, with alignment and positioning of these subunits into designed assemblies accomplished with the help of external forces and/or confined spatial templates. Additionally, stable connections between individual subunits in a given assembly have been achieved by using chemical crosslinkers,^[1] biomolecular interactions,^[2,5] or thermal fusion.^[15,16] However, the use of prefabricated subunits limits both the level of manufacturing integration and the functional capabilities of the resulting assemblies. For example, the use of solid particles prevents the incorporation of additional encapsulants into the final assemblies. Also, the use of thermal fusion to fix the subunits necessitates complicated device requirements while also being incompatible with the integration of biologically active components. Similarly, the use of chemical crosslinkers to connect prefabricated subunits demands that chemical handles be available on the subunits, thereby constraining the range of possible subunit materials or necessitating additional preprocessing steps with the subunits. To overcome these limitations, new techniques are needed that enable facile generation of subunits as well as their subsequent connection within an assembly.

Recently, microfluidics has emerged as a promising platform for the synthesis and assembly of microscale particles. While much research has been focused on the generation of microparticles,^[17–22] microfluidics can also provide a potential manufacturing paradigm at the microscale.^[12–16] First, nearly monodisperse subunits with precise and tunable size can be generated in a continuous process,^[23] and different payloads can be readily encapsulated within these subunits.^[19–22] Confined microfluidic channels can provide ideal spatial templates to anchor these subunits into complex assembly patterns, with stable intraparticle interactions achieved through the application of chemical or physical inputs.^[12–16] Moreover, the continuous nature of microfluidic particle generators offers the potential of realizing subunit generation, functionalization, and assembly all within a single microfluidic chip.

Herein, we present a microfluidic scheme that can both produce microsized subunits and connect these subunits within the same chip into complex multiparticle configurations. To illustrate the types of connected structures that can be produced, we focus on one-dimensional chains. Our subunits are microparticles of the biopolymer chitosan. This amino-polysaccharide has been intentionally selected because its primary amines allow for both intraparticle and interparticle crosslinking upon contact with dialdehydes such as glutaraldehyde (GA).^[24] We first generate monodisperse droplets by contacting an aqueous solution of chitosan at a microfluidic T-junction with a stream of hexadecane containing the detergent Span 80.^[23] These droplets are then interfacially crosslinked by a solution of GA injected through a tertiary channel. Robust chitosan microparticles of defined size are thus produced, and the functional properties of these particles are easily varied by including various payloads along with the chitosan solution, such as magnetic nanoparticles (MNPs) of $\gamma\text{-Fe}_2\text{O}_3$ and fluorescent water-soluble dyes.

We then demonstrate on-chip assembly of individual microparticles into permanently connected microchains. Here, we use the downstream microchannel as a spatial template

to confine the particles, and GA again serves as the chemical “glue” to link amine moieties on chitosan chains from adjacent particles. This allows us to generate chains of magnetic and/or fluorescent particles. Key notable points about our approach are the ability to control chain length with precision and the ability to control the arrangement of particles within a chain, for example, to generate chains with alternating fluorescent and nonfluorescent particles. In addition, chain flexibility can also be tuned by modulating the extent of GA-based crosslinking of adjacent particles (via the incubation time). Accordingly, we have created both rigid magnetic chains that can be rotated by an external magnetic field as well as semiflexible magnetic chains that show a beating motion in response to a magnetic field. Such magnetic chains are of interest for a variety of applications, for instance, as micromixers in microscale devices, as drug-delivery vehicles for magnetically targeted delivery, or as biomimetic microrobots.^[1,4]

Overall, our approach is distinct from other microfluidic manufacturing routes in that both subunit generation and subsequent connection are accomplished on the same chip and using the same chemistry. In contrast, in other approaches, subunit generation and assembly are usually carried out in separate steps with different chemistries in each step. Also, it should be noted that the chemicals used in this work are low-cost and commercially available, and no additional synthesis or purification steps are used. Finally, our microfluidic devices are based on the thermoplastic poly(methyl methacrylate) (PMMA), which makes the devices relatively cost-effective and easy to fabricate compared to those prepared from other substrate materials, such as glass and polydimethylsiloxane (PDMS).^[25–27] Thus, the above “micromanufacturing” process can potentially be scaled up for high-throughput production.

Fabrication of microfluidic devices from thermoplastic substrates can be significantly more efficient and cost-effective than PDMS microfabrication. Thermoplastic material costs are at least two orders of magnitude lower than those of PDMS. For small-volume production, thermoplastic channels with dimensions approaching 50 μm can be directly machined by micromilling, thereby obviating the need for photolithographic mold production, elastomer casting, and polymer curing. For mid-volume production, thermoplastics can be rapidly patterned by embossing from a micromachined mold with cycle times on the order of 10 min, while high-volume production can be achieved using exceptionally low cost reel-to-reel tape embossing methods.

2. Results and Discussion

2.1. Droplet Generation and Conversion to Robust Microparticles

Figure 1 shows a schematic of our microfluidic apparatus. The first element is the T-junction where the aqueous dispersed phase (2 wt% solution of chitosan) comes in contact with the nonpolar continuous phase (2 wt% solution of the detergent, Span 80 in hexadecane). As the dispersed phase is forced into the continuous phase, shear forces break

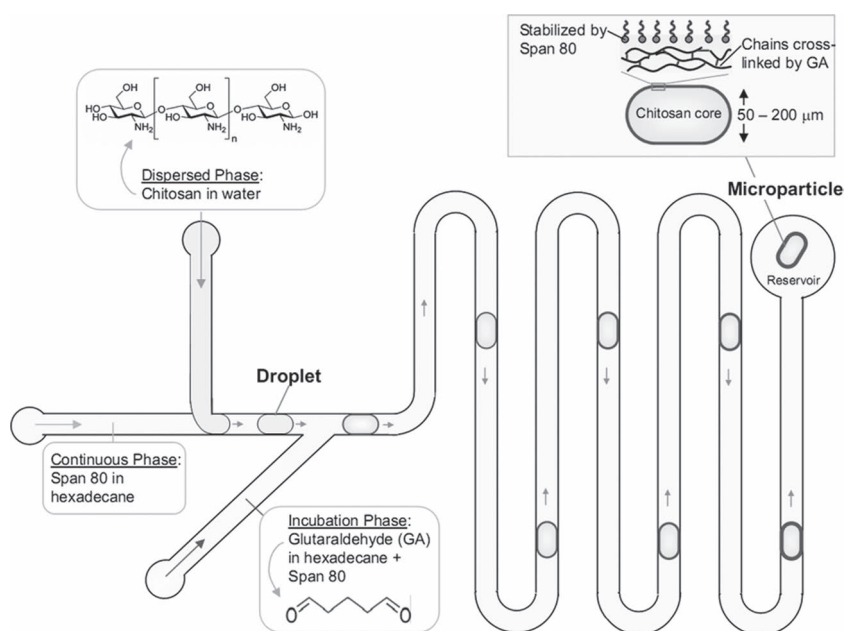


Figure 1. Microfluidic generation of chitosan microparticles. The channels have a rectangular cross section ($125\ \mu\text{m}$ height and $100\ \mu\text{m}$ width). At the T-junction, the dispersed phase (an aqueous chitosan solution) is contacted with the continuous phase (a solution of the detergent Span 80 in hexadecane), and in turn discrete aqueous droplets are formed. These droplets travel down the channel and meet the flow of the incubation phase, which consists of GA emulsified in hexadecane using Span 80. The GA crosslinks the droplets as they travel through the long, serpentine channel segment. Ultimately, the droplets are converted into particles and these are collected in the reservoir at the end. The inset shows a single microparticle: note that the chitosan chains are covalently linked by GA and the particle is stabilized in hexadecane by detergent molecules.

up the aqueous stream into a series of equally spaced droplets.^[23] The droplets are stabilized in the nonpolar continuous phase by Span 80 molecules, which are expected to arrange at droplet surfaces with their polar heads oriented inwards and their nonpolar tails pointing outwards into the external liquid (inset in Figure 1). The droplet size and generation frequency can be tuned to a desired value by adjusting the flow rates of the continuous and dispersed flows, or by adjusting the size of the microfluidic channel.^[23] In the present work, flow rates of $1.5\ \mu\text{L}\ \text{min}^{-1}$ for the continuous flow and $0.3\ \mu\text{L}\ \text{min}^{-1}$ for the dispersed flow were used to produce $\approx 150\text{-}\mu\text{m}$ -diameter droplets, with a typical generation speed of one droplet per second. This relatively slow generation rate was chosen to simplify the overall control of the system. However, higher generation speeds can be readily achieved within the same device by adjusting the total flow rates.

The second element in our microfluidic setup is the “incubation” stream, which is delivered through a side channel downstream from the T-junction to contact the droplets passing through the main channel (Figure 1). The incubation phase contains 2 wt% of GA emulsified into hexadecane using 2 wt% of Span 80 detergent. Note that GA is a bifunctional molecule, well known for its ability to react with the amine groups of chitosan and thereby crosslink chitosan droplets.^[24] When a chitosan-bearing droplet contacts the GA stream, GA molecules diffuse to the droplet and crosslink or “fix” the chitosan chains therein (inset in Figure 1). Similar crosslinking of droplets has been studied by Kumacheva et

al.^[17,19] for the case of alginate droplets in the presence of Ca^{2+} ions diffusing from the oil phase—the morphology of the resulting particles generally correlates with the concentration of crosslinkers. At low levels of crosslinker, the reaction is confined to the outer surface of the droplet and the resulting particle assumes a core/shell “microcapsule” structure. At higher levels of crosslinker, the entire droplet gets crosslinked and the particle is termed a “microbead” or “microgel”. For the case of our chitosan/GA system, we have observed that the contact (incubation) time between GA and chitosan droplets has a strong influence on the robustness of the resulting particles. To increase the incubation time, we positioned a long serpentine channel segment downstream from the GA injection point. For typical flow rates of $1.5\ \mu\text{L}\ \text{min}^{-1}$ for both the continuous and incubation streams (corresponding to about one droplet per second), an incubation time of $\approx 3\ \text{min}$ was found to be sufficient to convert the droplets into robust microparticles. The microparticles were then collected from the reservoir located at the end of the incubation channel.

Besides their robustness, another interesting aspect of our microparticles is their geometrical anisotropy. Generally, when the droplets emerge from the T-junction, they are deformed into a pluglike shape due to the constraint placed by the channel walls. In the absence of GA crosslinking, the droplets regain their surface-minimizing spherical form once they fall into the reservoir. A bright-field optical image of uncrosslinked droplets collected in the reservoir and surrounded by the continuous phase of hexadecane is shown in Figure 2a. Note that the droplets are spherical and also note their low polydispersity. However, when the pluglike droplets are brought into contact with GA in the channel, the rapid crosslinking fixes their anisotropic shape and the resulting particles do not relax back into a spherical form in the reservoir. This is seen from Figure 2b, which is an image of GA-crosslinked microparticles in hexadecane. In addition, these crosslinked particles are stable enough to be transferred from hexadecane to deionized (DI) water, which is an important virtue for applications where compatibility with aqueous solutions is necessary. The transfer was done by filtering the contents of the reservoir through a nylon net filter ($30\ \mu\text{m}$ pore size), followed by rinsing of the residue with ethanol and DI water, and finally adding the rinsed residue to DI water. Figure 2c is an image of microparticles in DI water, and a close-up of a single particle is shown in Figure 2d. Note that these particles contained MNPs (see below), and the black spots in the image correspond to aggregates of the MNPs. We have also conducted scanning electron microscopy (SEM) on the chitosan microparticles, and the relevant images are shown

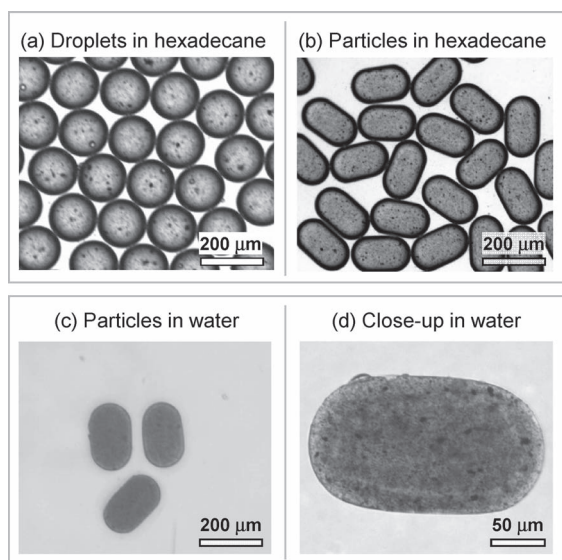


Figure 2. Optical images of a) spherical chitosan-bearing aqueous droplets in hexadecane (these were not contacted with GA); b) pluglike microparticles formed by crosslinking the above droplets with GA; c) the above microparticles transferred from hexadecane to DI water; and d) close-up of a single microparticle in water. Note that the droplets/particles contain MNPs, and the black spots in the images correspond to aggregates of these MNPs.

in Figure S1 (Supporting Information). The particles appear to be relatively homogeneous, which suggests that they are closer to microgels rather than microcapsules. Attempts to examine fracture surfaces by SEM were inconclusive, and this aspect requires further investigation.

2.2. Linking Microparticles into Microchains

Next, we describe our method for linking microparticles into chains. This method relies on the spatial confinement of particles in a microfluidic channel and GA–chitosan crosslinking to connect adjacent microparticles. We flow the microparticles into a channel and use a stainless steel wire

($\approx 60 \mu\text{m}$ diameter) to partially block the channel outlet (**Figure 3a**). The particles are thus trapped within the channel while the flow of solution around them continues. To avoid excessive pressure buildup, we stop the continuous and dispersed flows and reduce the incubation flow rate to $0.03 \mu\text{L min}^{-1}$. Successive microparticles are allowed to add onto the tail of the growing chain until the desired chain length is reached. In the process, individual subunits are brought into close proximity, thus allowing GA to form interparticle covalent bonds between chitosan chains on each pair of adjacent particles. Figure 3b is an optical image showing a particle chain in the channel. In addition, an image of a chain formed from smaller particles is shown in Figure S2 (Supporting Information). The extent of coupling between particles is determined by the GA contact time (i.e., the time over which the channel outlet is blocked). The flexibility of the chain can be controlled by varying this contact time, as further discussed in the next section. A key feature of our approach is the control over chain length. When the desired number of subunits has been connected into a robust chain, the chain is flushed into the reservoir, as shown in Figure 3a. We have found that a contact time of 5 min is sufficient to form a robust chain that does not fall apart in the reservoir. The above process can be easily replicated to generate multiple chains possessing precise lengths.

Furthermore, we demonstrated the ability to combine multiple building blocks within the same structure with precise control over their subunit arrangement. For this we modified the design of our microfluidic chip to feature two inlets for different dispersed phases (**Figure 4a**). We used a mixture of 2% chitosan and 0.1% of the water-soluble fluorescent dye, sodium fluorescein for dispersed phase 1, whereas dispersed phase 2 contained 2% chitosan only. When the flow rates of the two dispersed phases are the same (typical value: $0.3 \mu\text{L min}^{-1}$), the microparticles flowing down the main channel alternate between fluorescent and nonfluorescent ones. Such a microparticle train was blocked off, as shown before in Figure 3a, by the steel wire to enable interparticle connections to form during contact with GA. This process eventually results in a connected chain of alternating subunits. The alternating structure is clearly seen from the fluorescence image in Figure 4b, where every second subunit in the chain shows

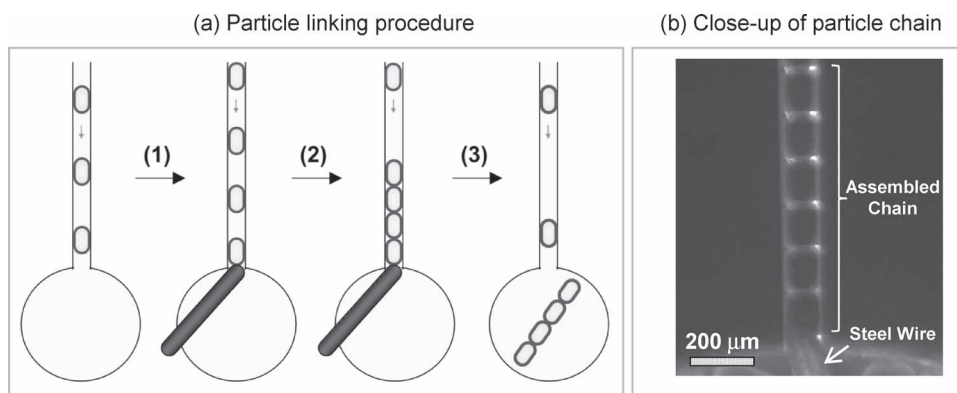


Figure 3. a) Schematic depiction of the on-chip process for linking individual particles into chains. 1) A stainless steel wire is used as a valve to block the channel outlet, 2) the wire is held until the desired number of subunits has been accumulated on the chain, and 3) the wire is then removed and the chain is flushed into the reservoir. b) Optical image showing a close-up of the assembled chain inside the microchannel.

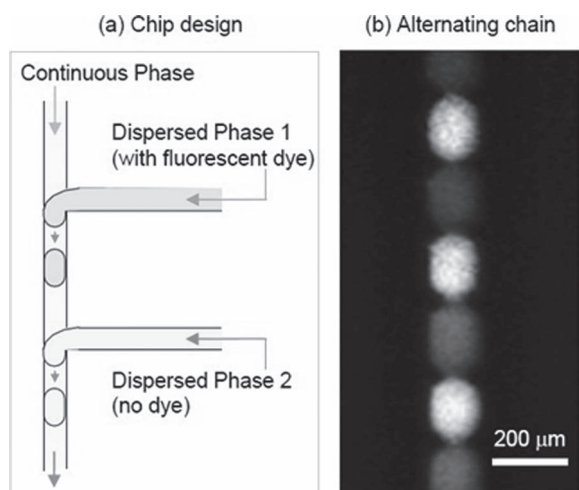


Figure 4. a) Schematic of the modified chip design used to prepare chains of alternating particles. The chip has two T-junctions corresponding to two dispersed phases. One dispersed phase has 0.1% of the fluorescent dye, sodium fluorescein, whereas the other does not contain dye. When the flow rates of the two dispersed phases are set equal, an alternating sequence of drops with and without the dye travel down the channel, where they are fixed into chains as described in Figure 3. b) Fluorescence image showing a particle chain with alternating fluorescent and nonfluorescent subunits.

bright fluorescence compared to its nearest neighbors. Other variations in chain structure, for example, where every n th microparticle in the chain is fluorescent, can also be prepared by simply controlling the relative flow rates of the two dispersed phases.

2.3. Magnetic Chains of Varying Flexibility

To further illustrate the possibilities inherent in our approach, we focused on a specific payload of interest, viz. MNPs of $\gamma\text{-Fe}_2\text{O}_3$. By encapsulating MNPs, we can impart magnetic properties to the individual microparticles. Towards this end, we mixed 0.5 wt% of the MNPs with the 2 wt% chitosan solution and used this mixture as the dispersed

phase. Interestingly, the MNPs did not remain well dispersed for long times in the chitosan solution—the fluid appeared homogeneous but microsized clumps could be seen by optical microscopy (as noted in Figure 2d). The clumping could be minimized by vigorous sonication of the dispersed phase before injection into the microfluidic device. At any rate, once the MNPs were encapsulated in the core of the chitosan microparticles, the clumping was not an issue with regard to the magnetic behavior of the microparticles. We confirmed that individual microparticles containing the MNPs could be magnetically manipulated using external bar magnets.

We then proceeded to create chains of magnetic particles using the procedure described above. First, we made stiff chains; in this case, the assembly was incubated for 24 h inside the channel to allow extensive interparticle connections via GA. The magnetic response of a stiff, three-member-long magnetic chain is demonstrated in **Figure 5** (these subunits also contained the fluorescent dye and the images were taken with a fluorescence microscope). For these experiments, the chain was transferred out of the microchannel and was placed in a petri dish. A permanent bar magnet was positioned a few centimeters above in an orientation parallel to the chain. When the external magnet was rotated from its original axis, the particle chain correspondingly rotated, as shown in Figure 5. Note that the assembled chain itself does not possess an intrinsic dipole to enable rotational control. Instead, the process results from interactions between the encapsulated MNPs. Under a constant magnetic field, each MNP establishes an individual magnetic dipole aligned to the applied field. Interactions between these dipoles generate a distribution of forces that exert a net torque on the chain until the chain's axis is aligned to the applied field. Similarly, translational motion of the magnetic chain may be realized by positioning one pole of the bar magnet closer to the assembled chain than the opposite pole. The magnetic control of longer rigid chains containing 30–40 subunits has also been realized (see Supporting Information, Figure S3).

The stiffness of the fabricated chains can be controlled by adjusting the contact (incubation) time of the chitosan microparticles with GA inside the blocked channel. Note that GA enhances both the degree of intraparticle crosslinking, which

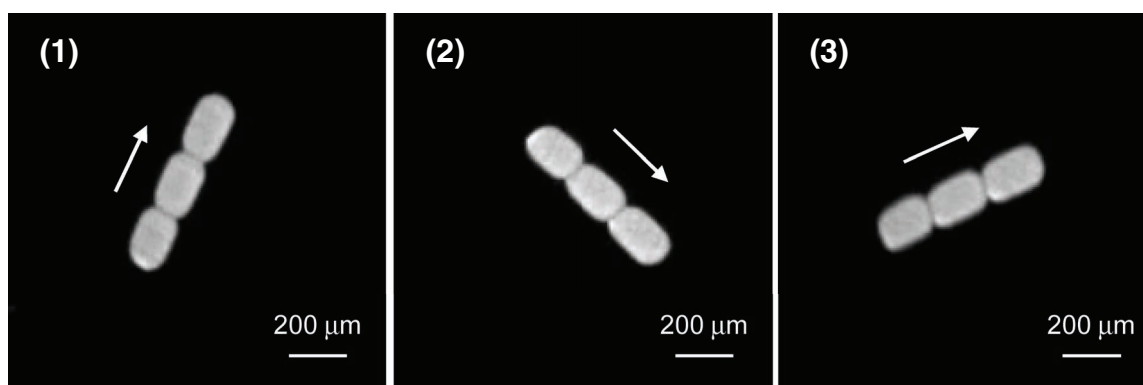


Figure 5. Rotation of a rigid magnetic chain when a bar magnet is rotated above the holding container. The chain is formed by extensive fusion of three chitosan particles bearing MNPs and a fluorescent dye. 1) to 3) represent successive images taken using a fluorescence microscope. Arrows indicate the direction of the net (induced) magnetic dipole at each instant.

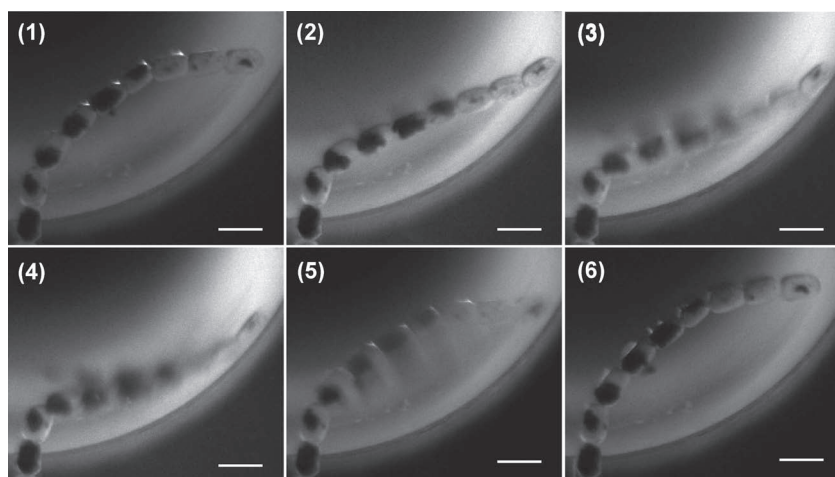


Figure 6. Undulating or “beating” motion of a semiflexible magnetic chain when a magnet is swayed on top of the holding container. 1) to 6) represent successive images obtained using a bright-field optical microscope. Scale bars: 200 μm . The above behavior can also be seen in Movie 1 (Supporting Information).

dictates the inherent modulus of the resulting chain, and the degree of interparticle crosslinking, which defines the rigidity of the interface between adjacent particles. While the relative influence of these factors is still under investigation, it is clear that long incubation times (≈ 24 h) lead to stiff rodlike chains, as shown above. In contrast, a moderate incubation time of ≈ 5 min produces flexible but mechanically robust chains. As illustrated by **Figure 6**, such semiflexible magnetic chains exhibit an undulatory (“beating”) motion when the orientation of an external magnetic field is changed. The undulatory motion of the chains can also be observed in Movie 1 (see Supporting Information).

2.4. Future Outlook

The broad approach of microfluidic assembly presented herein can be extended in a number of ways. For example, one could vary the net magnetic property of a chain by alternating magnetic and nonmagnetic subunits or by letting every fifth or tenth unit be a magnetic microparticle. One could also make chains of microparticles that are both magnetic and fluorescent to varying degrees, such as a chain with alternating magnetic and fluorescent units. Such an alternating arrangement of subunits may be of interest in the context of chemical and biological sensing.^[28] Lastly, in addition to linear chain assemblies, a variety of other shapes can be constructed using our microfluidic approach. One example is a Y shape of connected microparticles, which can be formed by branching the main channel into two and blocking off these branches to allow interparticle linking. This and other structures are being studied as part of ongoing work in our laboratory and will be reported in future papers. We believe our overall assembly approach of using chitosan microparticles as building blocks and connecting them with precision into larger structures is likely to be of considerable interest among scientists and engineers.

3. Conclusion

We have formed soft microparticles within a microfluidic device by contact of chitosan-bearing aqueous drops with a mixture of GA in hexadecane. These particles have low polydispersity and can be redispersed into DI water. The microparticle properties can be readily altered by varying the payloads included along with the initial chitosan solution: here, by using MNPs and fluorescent dyes we obtain magnetic and/or fluorescent particles. We then used these particles as building blocks for the construction of chains. To form chains on-chip, the microparticles are brought into close contact within a microchannel and incubated with a GA solution, whereupon the GA covalently links chitosan chains from adjacent particles. The chain length as well as the arrangement of particles within

a chain can be precisely controlled. Chain flexibility can also be tuned via the incubation time of the chain with GA—both rigid and semiflexible magnetic chains have been prepared by this approach. Overall, we suggest that microfluidic chips could serve as futuristic micromanufacturing platforms in which building blocks could be synthesized and then subsequently connected and positioned into complex and useful structures.

4. Experimental Section

Materials and Chemicals: Chitosan (medium molecular weight, 190–310 K; degree of deacetylation $\approx 80\%$) was obtained from Sigma–Aldrich. Magnetic $\gamma\text{-Fe}_2\text{O}_3$ nanoparticles (average surface area $\approx 42\text{ m}^2\text{ g}^{-1}$) were purchased from Alfa Aesar. The water-soluble fluorescent dye sodium fluorescein, the nonionic detergent sorbitan monooleate (Span 80), the nonpolar solvent hexadecane, and the crosslinking reagent GA (grade I, 50%) were obtained from Sigma–Aldrich. All chemicals were used as received. Rectangular neodymium bar magnets were obtained from McMaster Carr and nylon net filters (pore size, 30 μm) were purchased from Millipore.

Solution Preparation: Chitosan (2 wt%) was dissolved in acetic acid (0.2 M) solution. For magnetic and fluorescent capsule generation, $\gamma\text{-Fe}_2\text{O}_3$ nanoparticles (0.5 wt%) and fluorescein dye (0.1 wt%) were added to this solution, followed by vortex mixing and sonication. The final mixture is referred to as the “dispersed” phase. The “continuous” phase was prepared by dissolving Span 80 (2 wt%) in hexadecane. Finally, the “incubation” phase was a solution in hexadecane containing Span 80 (2 wt%) and GA (2 wt%). The above mixture was vortexed and sonicated before use.

Microfluidic Chip Fabrication and Operation: The microfluidic chip comprised a PMMA substrate (4” \times 2” \times 1/16”) containing microchannels bonded to a PMMA lid having access ports.^[27] PMMA sheets (FF grade; 4” \times 4” \times 1/16”) were purchased from Piedmont Plastics. The microchannels were fabricated by mechanical milling using an end mill (125 μm diameter) on a CNC milling machine with a depth of 100 μm . Holes for the needle interface and access reservoir were drilled into the substrate plate using a 650- μm -diameter

drill bit and a 2-mm-diameter drill bit, respectively. The machined PMMA plate was sequentially cleaned by DI water and isopropyl alcohol to remove the milling debris, followed by a 24 h degassing step in a 40 °C vacuum oven to remove the residual solvents. After vacuum drying, both the processed PMMA and a raw PMMA chip were oxidized by 8 min of exposure to ultraviolet light in the presence of ozone.^[25] The oxidized PMMA wafers were immediately mated together and thermally bonded at 85 °C in a hot press under a pressure of 3.45 MPa for 15 min. The world-to-chip interfaces were established by inserting hypodermic stainless steel needles into the 650- μ m-diameter mating holes, with an additional 30 min of annealing at 85 °C to release the residual stresses from the fitting process.^[29] Commercial microfluidic fittings (Upchurch) were used to connect the needle ports on the PMMA chip with off-chip fused silica capillaries, which were further connected to syringes. Precision syringe pumps (PHD 2000, Harvard Apparatus) were used to control the infusion of fluids into the chip. Optical detection was performed using either a Nikon Eclipse LV-100 profilometer microscope or a Nikon Eclipse TE2000s inverted fluorescence microscope.

Supporting Information

Supporting Information is available from the Wiley Online Library or from the author.

Acknowledgements

S.R.R. acknowledges the suggestions and input of graduate students Matthew Dowling and Khyati Tiwari during the initial stages of this work.

- [1] E. M. Furst, C. Suzuki, M. Fermigier, A. P. Gast, *Langmuir* **1998**, *14*, 7334.
- [2] S. L. Biswal, A. P. Gast, *Phys. Rev. E* **2003**, *68*.
- [3] S. L. Biswal, A. P. Gast, *Phys. Rev. E* **2004**, *69*.
- [4] S. L. Biswal, A. P. Gast, *Anal. Chem.* **2004**, *76*, 6448.
- [5] R. Dreyfus, J. Baudry, M. L. Roper, M. Fermigier, H. A. Stone, J. Bibette, *Nature* **2005**, *437*, 862.
- [6] S. Sacanna, W. T. M. Irvine, P. M. Chaikin, D. J. Pine, *Nature* **2010**, *464*, 575.
- [7] Y. D. Yin, Y. Lu, B. Gates, Y. N. Xia, *J. Am. Chem. Soc.* **2001**, *123*, 8718.
- [8] Y. D. Yin, Y. N. Xia, *J. Am. Chem. Soc.* **2003**, *125*, 2048.
- [9] Y. N. Xia, Y. D. Yin, Y. Lu, J. McLellan, *Adv. Funct. Mater.* **2003**, *13*, 907.
- [10] H. K. Wu, V. R. Thalladi, S. Whitesides, G. M. Whitesides, *J. Am. Chem. Soc.* **2002**, *124*, 14495.
- [11] S. H. Kim, S. J. Jeon, G. R. Yi, C. J. Heo, J. H. Choi, S. M. Yang, *Adv. Mater.* **2008**, *20*, 1649.
- [12] M. Bouquy, C. Serra, N. Berton, L. Prat, G. Hadziioannou, *Chem. Eng. J.* **2008**, *135*, S93.
- [13] H. Singh, P. E. Laibinis, T. A. Hatton, *Langmuir* **2005**, *21*, 11500.
- [14] A. B. Subramaniam, M. Abkarian, H. A. Stone, *Nat. Mater.* **2005**, *4*, 553.
- [15] K. E. Sung, S. A. Vanapalli, D. Mukhija, H. A. Mckay, J. M. Millunchick, M. A. Burns, M. J. Solomon, *J. Am. Chem. Soc.* **2008**, *130*, 1335.
- [16] S. A. Vanapalli, C. R. Iacovella, K. E. Sung, D. Mukhija, J. M. Millunchick, M. A. Burns, S. C. Glotzer, M. J. Solomon, *Langmuir* **2008**, *24*, 3661.
- [17] H. Zhang, E. Tumarkin, R. Peerani, Z. Nie, R. M. A. Sullan, G. C. Walker, E. Kumacheva, *J. Am. Chem. Soc.* **2006**, *128*, 12205.
- [18] J. L. Steinbacher, D. T. McQuade, *J. Polym. Sci. Polym. Chem.* **2006**, *44*, 6505.
- [19] H. Zhang, E. Tumarkin, R. M. A. Sullan, G. C. Walker, E. Kumacheva, *Macromol. Rapid Commun.* **2007**, *28*, 527.
- [20] A. Jahn, J. E. Reiner, W. N. Vreeland, D. L. DeVoe, L. E. Locascio, M. Gaitan, *J. Nanoparticle Res.* **2008**, *10*, 925.
- [21] D. Dendukuri, P. S. Doyle, *Adv. Mater.* **2009**, *21*, 4071.
- [22] E. Tumarkin, E. Kumacheva, *Chem. Soc. Rev.* **2009**, *38*, 2161.
- [23] D. R. Link, S. L. Anna, D. A. Weitz, H. A. Stone, *Phys. Rev. Lett.* **2004**, *92*.
- [24] S. R. Jameela, A. Jayakrishnan, *Biomaterials* **1995**, *16*, 769.
- [25] C. W. Tsao, L. Hromada, J. Liu, P. Kumar, D. L. DeVoe, *Lab Chip* **2007**, *7*, 499.
- [26] C. F. Chen, J. K. Liu, C. C. Chang, D. L. DeVoe, *Lab Chip* **2009**, *9*, 3511.
- [27] S. Yang, J. K. Liu, C. S. Lee, D. L. DeVoe, *Lab Chip* **2009**, *9*, 592.
- [28] C. F. Chen, J. Liu, L. P. Hromada, C. W. Tsao, C. C. Chang, D. L. DeVoe, *Lab Chip* **2009**, *9*, 50.
- [29] B. Zheng, J. D. Tice, R. F. Ismagilov, *Anal. Chem.* **2004**, *76*, 4977.

Received: March 16, 2011
 Revised: April 21, 2011
 Published online: June 28, 2011

NANO MICRO
small

Supporting Information

for *Small*, DOI: 10.1002/sml.201100514

A New Approach to In-Situ “Micromanufacturing”: Microfluidic Fabrication of Magnetic and Fluorescent Chains Using Chitosan Microparticles as Building Blocks

Kunqiang Jiang, Chao Xue, Chanda Arya, Chenren Shao, Elijah O. George, Don L. DeVoe,* and Srinivasa R. Raghavan*

Supporting Information for

DOI: 10.1002/smll.201100514

A New Approach to In Situ “Micro-Manufacturing”: Microfluidic Fabrication of Magnetic and Fluorescent Chains Using Chitosan Microparticles as Building Blocks

Kunqiang Jiang, Chao Xue, Chanda Arya, Chenren Shao, Elijah O. George, Don L. DeVoe, and Srinivasa R. Raghavan**

Keywords: Microfluidics, Chitosan, Microparticle, *In-situ* Assembly, Microchain

Experimental Section:

Scanning Electron Microscopy (SEM). SEM experiments on chitosan microparticles were conducted on a Hitachi SU-70 instrument at an accelerating voltage of 5 kV. The microparticles were washed with methanol 5 times, dispersed onto carbon black tape and dried under vacuum. They were then coated with gold for SEM imaging.

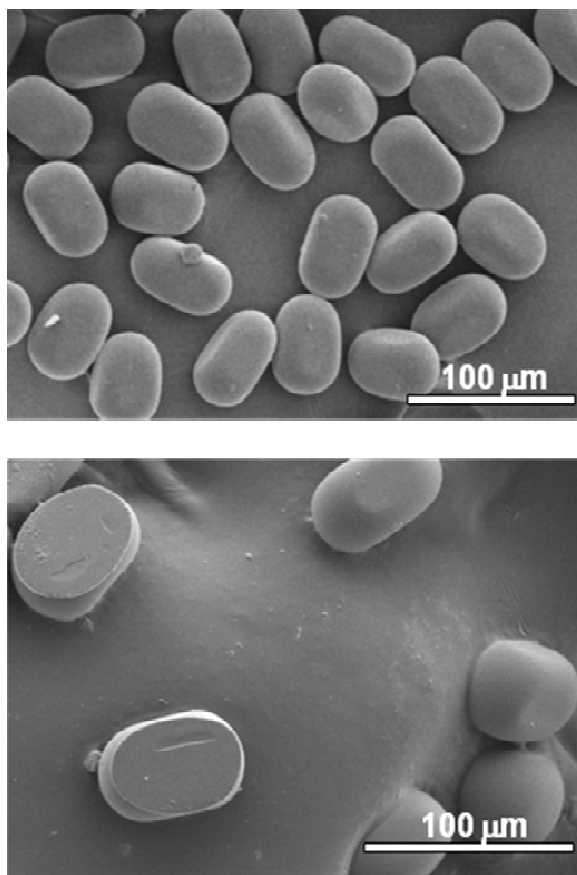


Figure S1: SEM micrographs of GA-crosslinked chitosan microparticles (similar to those seen in Figure 2c via optical microscopy). The particles have the plug shape seen also in Figure 2c. In the bottom image, a couple of broken particles are seen. These particles appear to have a gelled core, although one cannot rule out a core-shell morphology with different extents of crosslinking in the core and the shell.

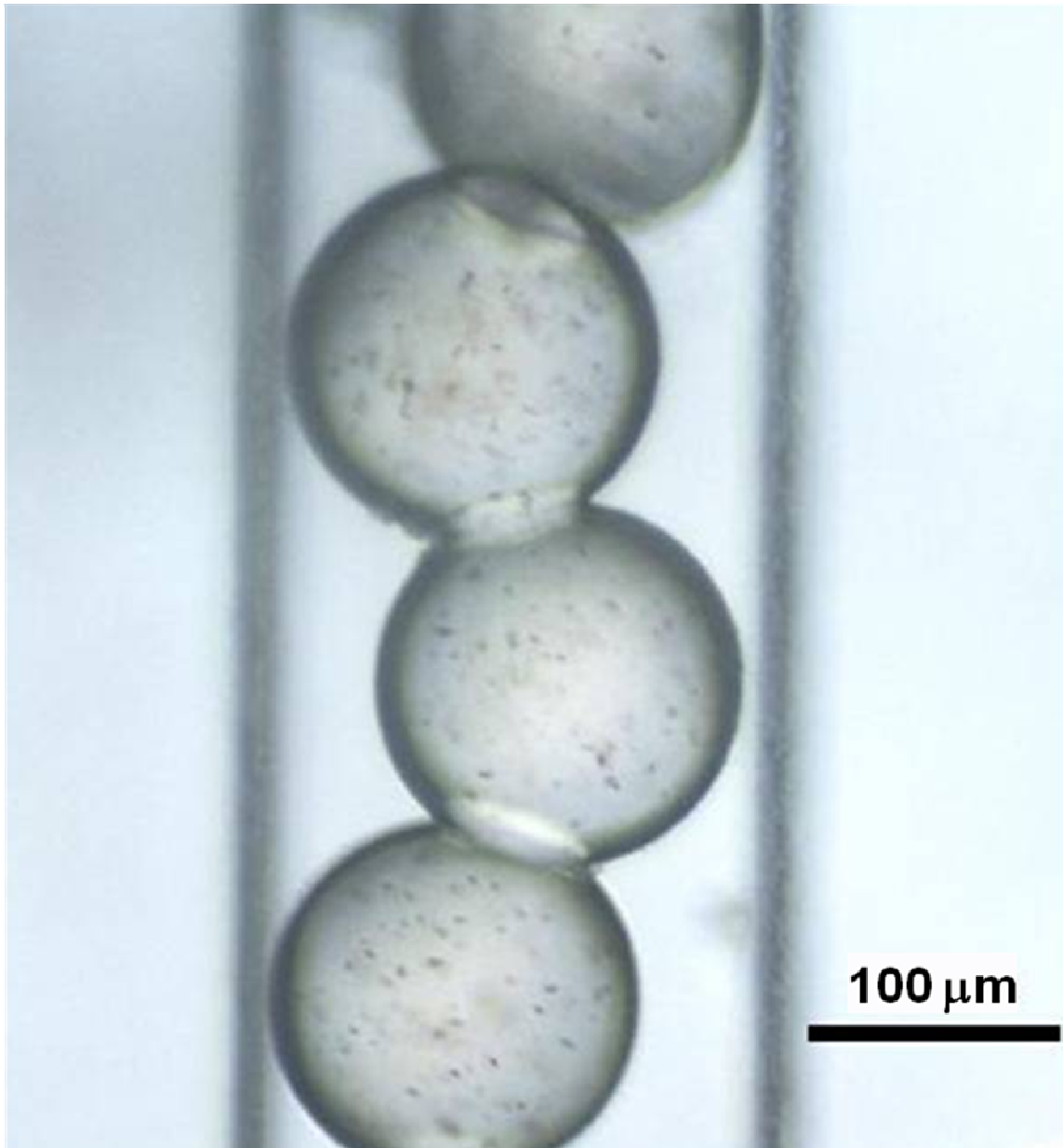


Figure S2: Magnetic chain formed by linking MNP-bearing chitosan subunits with a diameter of $\sim 140 \mu\text{m}$. Note that in this case, the subunits are smaller than the channel width, which is $200 \mu\text{m}$. As a result, the subunits retain their spherical shape in the linked chain. However, because the channel is an imprecise spatial template, the chain has a zig-zag shape.

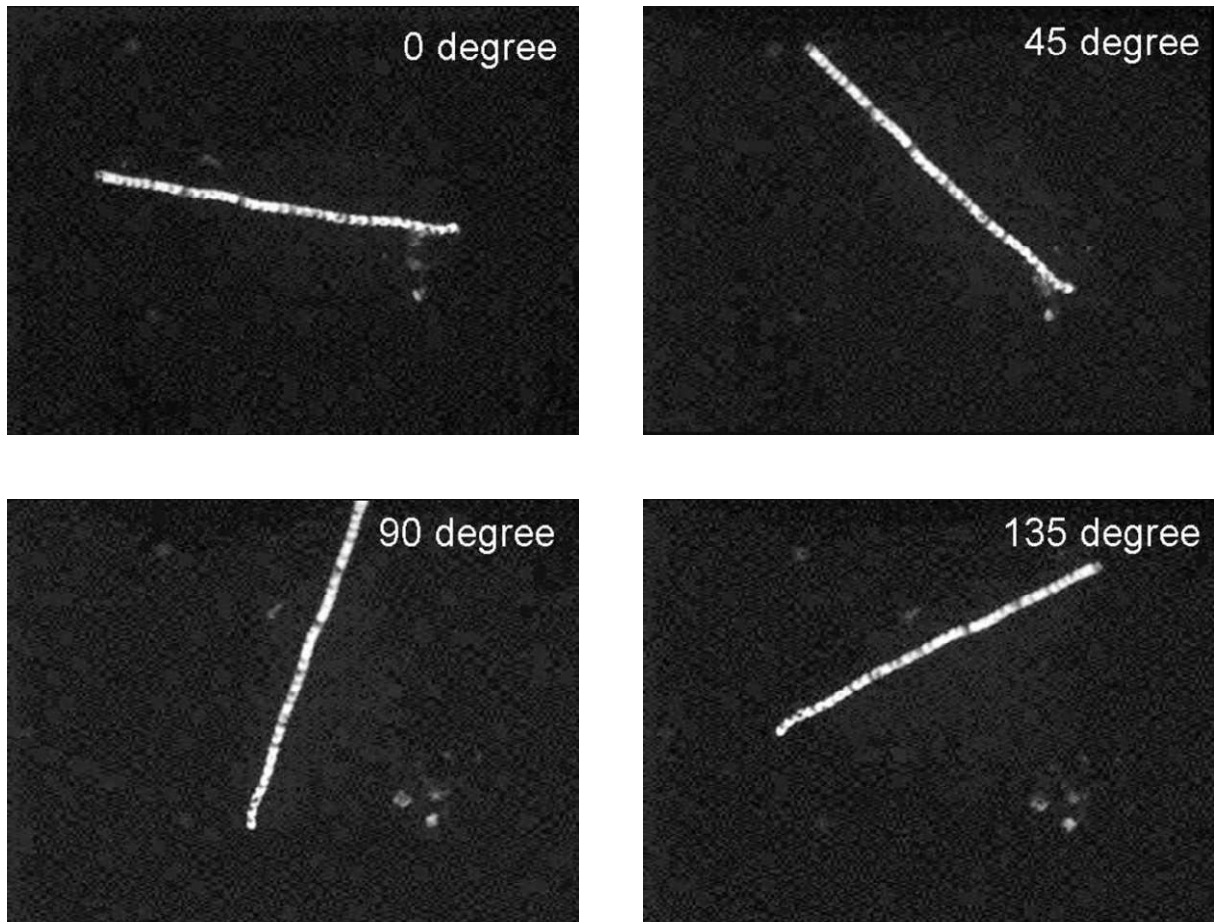


Figure S3: Magnetic manipulation of a long, rod-like chain synthesized by connecting 30-40 subunits on-chip, as shown in Figure 3. The subunits are chitosan microparticles containing MNPs.